Back to Einstein: how to include burial in fluvial sediment diffusion models?

James K. Pierce [1]**and Marwan A. Hassan**[1]

[1]Department of Geography
University of British Columbia

Key Points:

- We develop a random-walk model of objects in intermittent transport through an environment with traps.
- Its solution provides three ranges of diffusion, two of which are anomalous.
- We apply the model to sediment transport in rivers to clarify the scale-dependence of bedload diffusion.

Corresponding author: James Kevin Pierce, kpierce@alumni.ubc.ca

Abstract

In gravel-bed rivers, sediment grains transport through a sequence of motions and rests. When grains rest on the surface, they can be buried by material deposited from upstream. Buried grains are not exposed to the fluid flow, so these grains are immobile for relatively long periods, only becoming mobile once they're uncovered. This crucially affects the transport characteristics of sediment. Despite the importance of sediment burial to diffusion, very few models have accounted for it. In this letter, we develop a random-walk model to incorporate sediment burial. The model predicts three ranges of sediment diffusion with distinct characteristics in each range. We express the crossover times between these ranges in terms of measurable transport parameters, and explain each range in terms of underlying physical processes. This provides new geophysical understanding of the scale-dependent phenomenon of fluvial sediment transport.

1 Introduction

Anomalous diffusion has been the topic of intense research lately, since it appears in contexts as diverse and important as the transport of cholesterols through lipid bilayers (Jeon, Monne, Javanainen, & Metzler, 2012; Molina-Garcia et al., 2018), contaminants through soils (Berkowitz, Cortis, Dentz, & Scher, 2006; X. R. Yang & Wang, 2019), and pollinator insects through ecosystems (Reynolds & Rhodes, 2009; Vallaeys, Tyson, Lane, Deleersnijder, & Hanert, 2017). Emerging research in fluvial geomorphology has come to anomalous diffusion as well, since coarse sediment grains transporting through river channels apparently display it (Bradley, 2017; Martin, Jerolmack, & Schumer, 2012). H. A. Einstein (1937) developed the first model of fluvial bedload diffusion, which is the spreading apart of grains as they transport downstream. Diffusion is induced by differences in the transport characteristics of one grain and the next, and it is usually quantified by the time-dependence of the positional variance $\sigma_x^2(t)$ of a population. When $\sigma_x^2 \propto t$, the diffusion is said to be normal, since this is found in the classic diffusion problems (e.g. A. Einstein, 1905; Taylor, 1920). However, many transport phenomena show $\sigma_x^2 \propto t^\gamma$, with $\gamma \neq 1$. This diffusion is said to be anomalous (Sokolov, 2012). If $\gamma > 1$, it is said to be superdiffusive; while if $\gamma < 1$, it is said to be subdiffusive (Metzler & Klafter, 2000).

Researchers after Einstein have come to recognize that coarse sediment moving through river channels can show either anomalous or normal diffusion depending on the timescale of observation (Nikora, 2002). This is a significant issue since it implies diffusion models should be scale dependent, and it renders experimental data contingent on their observation timescales. Nikora (2002); Nikora, Heald, Goring, and McEwan (2001) first identified three ranges of bedload diffusion from simulations and experimental data, and they termed these local, intermediate, and global ranges in order of increasing scale. σ_x^2 scales with a different power of time in each range, and this scaling can be anomalous or normal. Their findings are supported by a wide set of contemporary data and numerical simulations that show up to three ranges of bedload diffusion (Bialik, Nikora, & Rowiński, 2012; Bradley, 2017; Fan, Singh, Guala, Foufoula-Georgiou, & Wu, 2016; Martin et al., 2012; Wu et al., 2019; Zhang, Meerschaert, & Packman, 2012). While earlier works have developed models of bedload diffusion, there are contradictions in the literature about the expected diffusion characteristics (super/normal/subdiffusion) of each range, and no model has been developed, to our knowledge, that derives all three diffusion ranges from process-based concepts of fluvial sediment transport.

In this letter, we present a model of bedload diffusion which describes local, intermediate, and global ranges by including the duration of motion and the possibility of trapping due to burial into the classic bedload diffusion model of H. A. Einstein (1937). Einstein's model has been highly influential in river geophysics and has fostered

an entire paradigm of research that leverages and generalizes his stochastic methods (e.g. Gordon, Carmichael, & Isackson, 1972; Hubbell & Sayre, 1964; Nakagawa & Tsujimoto, 1976; C. T. Yang & Sayre, 1971; Yano, 1969). Its essential content is that individual grains move in instantaneous steps interrupted by durations of rest which lie on statistical distributions (Hassan, Church, & Schick, 1991). It predicts a single range of normal diffusion (H. A. Einstein, 1937; Nakagawa & Tsujimoto, 1976). Essentially, the Einstein model is a special case of the continuous time random walk (CTRW) (Montroll & Weiss, 1965), originally developed to describe anomalous diffusion of charge carriers in solids. To include the duration of motion and the burial process we leverage the multi-state generalization of the CTRW developed by Weiss (1976, 1994). Our development allows us to derive three ranges of diffusion and the scaling behavior of σ_x^2 in each range. The model is analytically solvable, and we determine the cross-over times between diffusion ranges. Several progressive works have discriminated multiple ranges of bedload diffusion due to the duration of motion (Lisle et al., 1998) and sediment burial (Wu et al., 2019), and multiple ranges of diffusion have been shown in models of other transport phenomena (e.g. Aarão Reis & Di Caprio, 2014; Balakrishnan & Chaturvedi, 1988; Bena, 2006; Flekkøy, 2017). However, we believe our proposed model is the first analytically solvable model of three diffusion ranges. We present the model in section 2 and solve it in section 3. We use the solution in section 4 to directly attribute physical processes to each diffusion range, to discern the crossover times between ranges in terms of empirically measurable transport parameters, and to derive earlier works as limiting cases (e.g. H. A. Einstein, 1937; Lisle et al., 1998; Wu et al., 2019).

2 Bedload diffusion with burial as a multi-state random walk

We use a three-state random walk where the states are motion, rest, and burial. We label these as $i = 2$ (motion), $i = 1$ (rest), and $i = 0$ (burial). Our development of the governing equations for the three-state walk closely mimics Weiss (1994), and our approach to incorporating the trapping process closely mirrors Schmidt, Sagués, and Sokolov (2007). In our model, residence times in motion and rest states are random variables characterized by exponential distributions and motions are characterized by a constant velocity v. We consider burial to be a permanent condition which has some probability to occur when resting grains are covered by transported sediment. The probability of burial per unit time (burial rate) is considered constant, so the probability of trapping increases with the time grains spend resting.

A central concept in our derivation is the idea of a sojourn in the state i (Weiss, 1994). When a grain enters a state i at some time t_0 and position x_0, then leaves a state at some other time t_1 and position x_1, we say that the grain has completed a sojourn in the state i. The joint probability density for a complete sojourn through the state i of time $t = t_1 - t_0$ and displacement $x = x_1 - x_0$ is denoted $g_i(x, t)$. Similarly, we can consider incomplete sojourns. If a grain begins a sojourn in the state i at (t_0, x_0) and the sojourn is still on-going, the joint probability density to find the grain at (x_1, t_1) is $G_i(x, t)$. The g_i and G_i can be further decomposed when time and space components of the motion are independent (Weiss, 1994). We refer to g_i and G_i as the complete and incomplete propagators, since they move probability through space-time and are associated respectively with complete and incomplete sojourns.

Our target is the probability distribution $p(x, t)$ to find a grain at x, t if we know it started at $(x, t) = (0, 0)$, that is, with the initial distribution $p(x, 0) = \delta(x)$. We denote the initial probabilities to be at rest or in motion as θ_1 and θ_2. Normalization requires $\theta_1 + \theta_2 = 1$. Our derivation has two main steps. First, we introduce and solve for a set of joint probabilities associated with transitions of a grain from one state to another. Second, we use these quantities to solve for the probabilities that a grain is

in state i having position x at time t. Afterward, we sum the these distributions over all states i to derive the joint probability that a grain is in any state at (x, t).

Now we begin the first stage of the derivation. Grains at rest may be trapped by burial. We consider burial to be permanent (e.g. Wu et al., 2019), and we assume resting grains may be buried with constant probability per unit time κ. Equivalently, we could say the mean time required for a resting grain to become buried is $1/\kappa$. From this assumption, the probability that a grain is not trapped after a time t at rest is given by a survival function $\Phi_F(t) = e^{-\kappa t}$ (F is for "free"). Likewise, the probability that it is trapped after resting for a time t is the complement $\Phi_T(t) = 1 - \Phi_F(t)$ (T is for "trapped"). We introduce $\omega_{1T}(x, t)$, $\omega_{1F}(x, t)$, and $\omega_2(x, t)$ as the joint probabilities to find a grain at (x, t) having just completed a sojourn. The subscript $1T$ denotes the completion of a rest sojourn due to trapping by burial, while $1F$ denotes the completion of a rest sojourn due to motion. Similarly, the subscript 2 denotes the completion of a motion sojourn due to resting. Using an argument similar to Weiss (1994), we write integral equations to link the ω's:

$$\omega_{1T}(x,t) = \theta_1 \Phi_T(t) g_1(x,t) + \int_0^x dx' \int_0^t dt' \omega_2(x',t') \Phi_T(t-t') g_1(x-x', t-t'), \quad (1)$$

$$\omega_{1F}(x,t) = \theta_1 \Phi_F(t) g_1(x,t) + \int_0^x dx' \int_0^t dt' \omega_2(x',t') \Phi_F(t-t') g_1(x-x', t-t'), \quad (2)$$

$$\omega_2(x,t) \quad = \theta_2 g_2(x,t) + \int_0^x dx' \int_0^t dt' \omega_{1F}(x',t') g_2(x-x', t-t'). \quad (3)$$

The first equation can be understood as follows: $\omega_{1T}(x, t)$ describes the probability that a sojourn in the state 1 ends due to trapping at (x, t). This quantity has two contributions. The first contribution represents the possibility that the grain started at $(x, t) = (0, 0)$ in the $i = 1$ state (with probability θ_1), propagated a distance x and a time t in the $i = 1$ state (with probability density $g_1(x, t)$), was trapped (with probability $\Phi_T(t)$), and is now at (x, t). The second contribution describes the possibility that the grain was in a motion sojourn which ended at x', t' when it came to rest. From here, it propagated from x', t' to x, t at rest (with probability density $g_1(x - x', t - t')$) and was trapped during this sojourn (with probability $\Phi_T(t - t')$). The other equations can be reasoned similarly; these arguments are analogous to Weiss (1994). Once the propagators are specified, we can solve (1-3) for the ω's. This completes the first stage of the derivation.

The second stage of our derivation involves the joint probabilities of being in state regardless of whether a sojourn has just completed. These are denoted by $p_0(x, t)$ (trapped), $p_1(x, t)$ (rest), and $p_2(x, t)$ (motion), and they involve the ω's for their definition:

$$p_0(x,t) = \int_0^t dt' \omega_{1T}(x, t-t'), \quad (4)$$

$$p_1(x,t) = \theta_1 G_1(x,t) + \int_0^x dx' \int_0^t dt' \omega_2(x',t') G_1(x-x', t-t'), \quad (5)$$

$$p_2(x,t) = \theta_2 G_2(x,t) + \int_0^x dx' \int_0^t dt' \omega_{1F}(x',t') G_2(x-x', t-t'). \quad (6)$$

Equation (4) says that grains buried at any (x, t) arrived there due to trapping at x at any time leading up to t. The reasoning in (5-6) is the same as for (1-3), except we use the propagators for incomplete sojourns. These equations can be solved once the propagators are specified and the ω's are known from (1-3). Finally, we form the total probability density for a grain to be found at (x, t) in any state. This is simply

$$p(x,t) = p_0(x,t) + p_1(x,t) + p_2(x,t). \quad (7)$$

This joint density is completely determined once (1-6) are solved.

3 Specification of propagators and solution of model

We consider sojourns in the rest state to occur for an exponentially distributed time interval, given by the distribution $\psi_1(t) = k_1 e^{-k_1 t}$. The probability that a sojourn in this state lasts for at least a time t is then given by $\Psi_1(t) = \int_t^\infty \psi_1(t)dt = e^{-k_1 t}$. $1/k_1$ is the mean duration of a single rest. Since grains do not move in the rest sojourn, the probability density that a grain is displaced by a distance x in the rest sojourn in $\delta(x)$. Hence the complete propagator for rest sojourns is $g_1(x,t) = \delta(x)\psi_1(t)$, or

$$g_1(x,t) = \delta(x)k_1 e^{-k_1 t}. \tag{8}$$

Likewise, the incomplete propagator for a rest sojourn is $G_1(x,t) = \delta(x)\Psi_1(t) = \delta(x)e^{-k_1 t} = g_1(x,t)/k_1$. The motion propagators are reasoned similarly. We consider motions to occur with a constant velocity v and to have an exponentially distributed duration given by $\psi_2(t) = k_2 e^{-k_2 t}$. $1/k_2$ is the mean duration of a single motion. Since the velocity of motions is deterministic, the probability to find a grain at position x in a motion sojourn is $\delta(x - vt)$, and the complete propagator for motion sojourns is

$$g_2(x,t) = \delta(x - vt)k_2 e^{-k_2 t}, \tag{9}$$

while the incomplete propagator is $G_2(x,t) = g_2(x,t)/k_2$ as before.

Having defined the propagators, we set out to solve (1-6) and understand bedload diffusion with a finite motion interval and when subject to trapping by burial. The convolution structure of equations (1-6) presents a formidable problem. Luckily, we have the device of Laplace transforms. These project integro-differential equations into an alternate space in which convolutions are unraveled (e.g. Arfken, 1985). The double Laplace transform of a joint probability distribution $p(x,t)$ is defined by

$$\tilde{p}(\eta, s) = \int_0^\infty dx e^{-\eta x} \int_0^\infty dt e^{-st} p(x,t). \tag{10}$$

The Laplace-transformed moments of x are linked to derivatives of the double-transformed distribution (10) (cf. Berezhkovskii & Weiss, 2002). From equation (10) it's clear that

$$\langle \tilde{x}(s)^k \rangle = (-)^k \partial_\eta^k \tilde{p}(\eta, s)\Big|_{\eta=0}. \tag{11}$$

The operator $\langle \circ \rangle$ denotes the ensemble average (e.g. Kittel, 1958). This means we can compute the variance of position as $\sigma_x^2(t) = \langle x^2 \rangle - \langle x \rangle^2 = \mathcal{L}^{-1}\{\langle \tilde{x}^2 \rangle; t\} - \mathcal{L}^{-1}\{\langle \tilde{x} \rangle; t\}^2$, where $\mathcal{L}^{-1}$ denotes the inverse Laplace transform (e.g. Arfken, 1985). This is a powerful tool, since we can use it to derive the positional variance without integrating the distribution in equation (7).

Using the propagators (8-9) and this transform calculus, the joint distribution $p(x,t)$ is derived in appendix A, while the moments $\langle x \rangle$ and $\langle x^2 \rangle$ and ultimately the variance of position $\sigma_x^2(t)$ are derived in appendix B. With the shorthand notations $\xi = k_2 x/v$, $\tau = k_1(t - x/v)$, and $\Omega = (\kappa + k_1)/k_1$ (cf. Lisle et al., 1998), the joint distribution to find a grain at position x at time t is

$$\begin{aligned} p(x,t) = \theta_1 \mathcal{H}(\xi)\mathcal{H}(\tau)\Big[1 - \frac{k_1}{\kappa + k_1}\Big(1 - e^{-(\kappa+k_1)t}\Big)\Big]\delta(x) \\ + \frac{1}{v} e^{-\Omega\tau - \xi}\mathcal{H}(\xi)\mathcal{H}(\tau)\Big(\theta_1\Big[k_1 \mathcal{I}_0\big(2\sqrt{\xi\tau}\big) + k_2\sqrt{\frac{\tau}{\xi}}\mathcal{I}_1\big(2\sqrt{\xi\tau}\big)\Big] \\ + \theta_2\Big[k_1\delta(\tau) + k_2\mathcal{I}_0\big(2\sqrt{\xi\tau}\big) + k_1\sqrt{\frac{\xi}{\tau}}\mathcal{I}_1\big(2\sqrt{\xi\tau}\big)\Big]\Big) \\ + \frac{1}{v}\frac{\kappa k_2}{\kappa + k_1} e^{-\kappa\xi/(\kappa+k_1)}\mathcal{H}(\xi)\mathcal{H}(\tau)\Big((\theta_1/\Omega)\mathcal{P}_2(\xi/\Omega, \Omega\tau) + \theta_2\mathcal{P}_1(\xi/\Omega, \Omega\tau)\Big). \end{aligned} \tag{12}$$

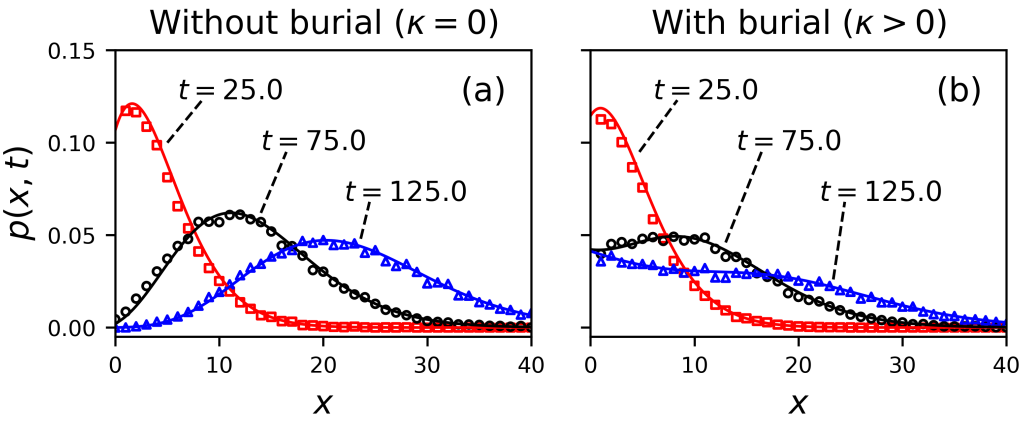

Figure 1. Joint distributions for a grain to be at position x at time t are displayed for the choice $k_1 = 0.1$, $k_2 = 1.0$, $v = 2.0$. Grains are considered initially at rest ($\theta_1 = 1$, $\theta_2 = 0$). The solid lines are the analytical distribution in equation (12), while the points are simulation results to show mathematical correctness. Colors pertain to different times. Units are unspecified, since our aim is to demonstrate the general characteristics of $p(x, t)$. Panel (a) shows the case $\kappa = 0$ – the absence of burial. In this case, the joint distribution tends toward Gaussian at large times (e.g. H. A. Einstein, 1937; Lisle et al., 1998). Panel (b) shows the case when grains have rate $\kappa = 0.01$ to become buried while resting. Because of burial, the joint distribution tends toward a more uniform distribution than Gaussian. This shows a redistribution of probability to smaller values of x due to the burial process (cf. Wu et al., 2019). The redistribution is encoded mathematically by the Marcum Q-function terms in equation (12). A similar tendency is seen in field studies of tracer dispersion in gravel bed rivers (e.g. Hassan & Church, 1994).

$\mathcal{H}$ is the Heaviside step function and we use the convention $\mathcal{H}(0) = 1$. The $\mathcal{I}_\nu$ are modified Bessel functions of the first kind, and the $\mathcal{P}_\mu$ are generalized Marcum Q-functions defined by $\mathcal{P}_\mu(x, y) = \int_0^y e^{-z-x}(z/x)^{(\mu-1)/2}\mathcal{I}_{\mu-1}(2\sqrt{xz})dz$ (Temme, 1996). Modified Bessel functions are common in one-dimensional diffusion problems (e.g. Daly & Porporato, 2010; H. A. Einstein, 1937; Giddings & Eyring, 1955).

The Marcum Q-functions are convolutions between modified Bessel functions and decaying exponentials. They were originally devised in relation to radar detection problems (Marcum, 1960). Conceptually, the Q-functions emerge in our context from the sediment burial process. According to our assumptions, resting grains can become buried in some interval of time with an exponential probability. Meanwhile, the probability that grains are resting follows a modified Bessel distribution (e.g. H. A. Einstein, 1937; Lisle et al., 1998). As a result, the probability that sediment is resting and becomes buried involves the convolution structure of the Marcum Q-functions. Consistent with this interpretation, the terms involving these convolutions vanish when the burial rate is taken to zero ($\kappa \to 0$). The distribution (12) is depicted in figure 1 alongside simulations generated by a direct method. This method is based on evaluating the cumulative transition probabilities between states on a small timestep (cf. Barik, Ghosh, & Ray, 2006). A link to the simulation code, which includes descriptive comments, is available in the acknowledgments.

The first two moments and the positional variance are derived in appendix B. The moments take the form

$$\langle x(t)\rangle = A_1 e^{(b-a)t} + B_1 e^{-(a+b)t} + C_1, \tag{13}$$

$$\langle x^2(t)\rangle = A_2(t) e^{(b-a)t} + B_2(t) e^{-(a+b)t} + C_2. \tag{14}$$

In these equations, $a = (\kappa + k_1 + k_2)/2$ and $b = \sqrt{a^2 - \kappa k_2}$ are effective rates having dimensions of inverse time. The A_i and B_i are polynomials available in table 1. The variance is

$$\sigma_x^2(t) = A(t) e^{(b-a)t} + B(t) e^{-(a+b)t} + C(t). \tag{15}$$

A, B, and C are transcendental functions available in table 1. This equation represents the scale-dependence of bedload diffusion for sediment gradually undergoing burial.

Table 1. Polynomials and transcendental functions used in the expressions of the mean (13), second moment (14) and variance (15) of bedload tracers.

$$A_1 = \frac{v}{2b}\Big[\theta_2 + \frac{k_1 + \theta_2\kappa}{b-a}\Big]$$

$$B_1 = -\frac{v}{2b}\Big[\theta_2 - \frac{k_1 + \theta_2\kappa}{a+b}\Big]$$

$$C_1 = -\frac{v}{2b}\Big[\frac{k_1 + \theta_2\kappa}{b-a} + \frac{k_1 + \theta_2\kappa}{a+b}\Big]$$

$$A_2(t) = \frac{v^2}{2b^3}\Big[(bt-1)[k_1 + \theta_2(2\kappa + k_1 + b - a)] + \theta_2 b + \frac{(\kappa + k_1)(\theta_2\kappa + k_1)}{(b-a)^2}[(bt-1)(b-a) - b]\Big]$$

$$B_2(t) = \frac{v^2}{2b^3}\Big[(bt+1)[k_1 + \theta_2(2\kappa + k_1 - a - b)] + \theta_2 b - \frac{(\kappa + k_1)(\theta_2\kappa + k_1)}{(a+b)^2}[(bt+1)(a+b) + b]\Big]$$

$$C_2 = \frac{v^2}{2b^3}(\kappa + k_1)(\theta_2\kappa + k_1)\Big[\frac{2b-a}{(b-a)^2} + \frac{a+2b}{(a+b)^2}\Big]$$

$$A(t) = A_2(t) - 2A_1C_1 - A_1^2 \exp[(b-a)t]$$

$$B(t) = B_2(t) - 2B_1C_1 - B_1^2 \exp[-(a+b)t]$$

$$C(t) = C_2 - C_1^2 - 2A_1B_1 \exp[-2at]$$

The positional variance is plotted in figure 2 for conditions $\theta_1 = 1$ and $k_2 \gg k_1 \gg \kappa$. These conditions mean that all grains are initially at rest (cf. Wu et al., 2019), motion intervals are typically much shorter than rests (cf. H. A. Einstein, 1937), and that sediment burial occurs over a much longer time than typical rests. We concentrate on these conditions in the discussion which follows as we believe they are most relevant to bedload diffusion in gravel bed rivers where sediment transport is mostly rarefied and intermittent (Frey, 2014) and the process of grains becoming buried while they rest on the surface is relatively slow (e.g. Hassan & Church, 1994). Figure 2 demonstrates that under these conditions the variance (15) shows three ranges of bedload diffusion with approximate power law scaling ($\sigma_x^2 \propto t^\gamma$) and a fourth range with no diffusion ($\sigma_x^2 = \text{const}$) that results from the burial of all sediment grains. We identify the first three ranges as similar to the local, intermediate, and global ranges proposed by Nikora (2002); Nikora et al. (2001). We suggest to call the fourth range the geomorphic range, since any further diffusion in this range would require scour of the bed (i.e., a geomorphic change) to expose buried grains to the flow (cf. Martin, Purohit, &

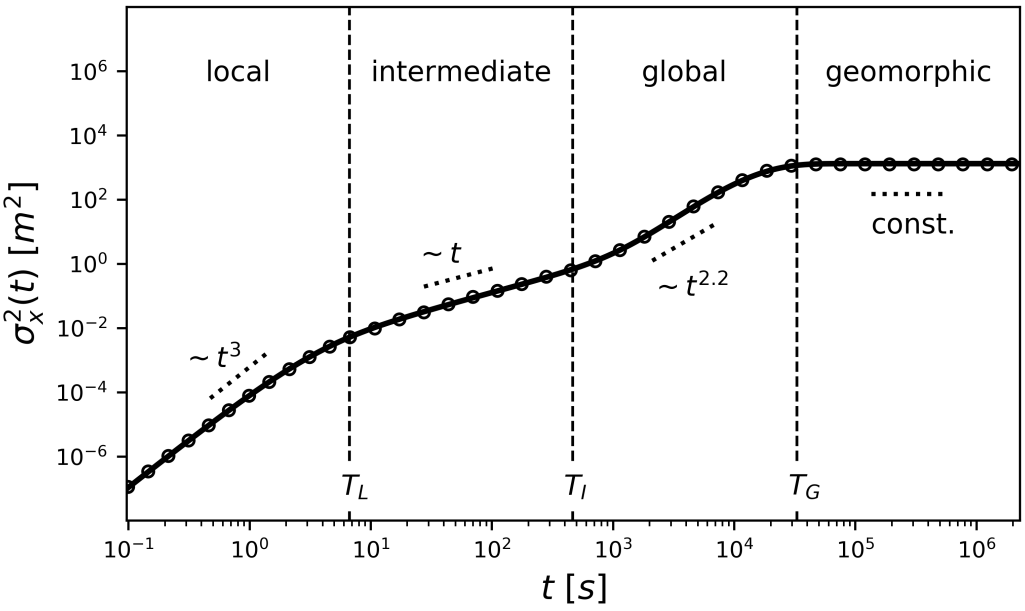

Figure 2. Bedload diffusion for the parameters $1/k_2 = 1.5$s, $1/k_1 = 30.0$s, and $v = 0.1$m/s. These values are comparable to laboratory flume experiments using small ($\sim$ 5mm) gravel (cf. Lajeunesse et al., 2010; Martin et al., 2012; Yano, 1969). The timescale of burial is $1/\kappa = 7200.0$s (two hours), and the initial condition is rest ($\theta_1 = 1$). The solid line is equation (15) while the points are directly simulated. When $k_2 \gg k_1 \gg \kappa$, as as is the case in this plot, there are four distinct scaling ranges of σ_x^2: local, intermediate, global, and geomorphic. Within each range, a slope key is added to demonstrate the scaling $\sigma_x^2 \propto t^\gamma$. There are three crossovers between these ranges, denoted on the figure by vertical lines. The crossover times are denoted T_L, T_I, and T_G. They are given in equations (16-18) in terms of the parameters of the model.

Jerolmack, 2014; Nakagawa & Tsujimoto, 1980; Voepel, Schumer, & Hassan, 2013). Using this terminology, we summarize that when $k_2 \gg k_1 \gg \kappa$ and $\theta_1 = 1$, the variance in equation (15) expresses four scaling ranges of bedload diffusion: local, intermediate, global, and geomorphic.

4 Discussion of scale-dependent bedload diffusion

The four range model of sediment diffusion we have presented requires four parameters. These are the characteristic velocity v of moving sediment and three key timescales: $1/k_2$, $1/k_1$, and $1/\kappa$. Respectively, these timescales represent the mean duration of motion, the mean duration of rest, and the mean duration sediment rests before it becomes buried. As shown in figure 2, the diffusion in the first three ranges is approximately characterized by scaling laws of the form $\sigma_x^2 \propto t^\gamma$. The exponents γ in each range result from competition between different terms in equation (15). Between these ranges, there are three crossover regions where the scaling is not a pure power law. Because these crossover regions are relatively narrow, we can characterize them with crossover times T_L, T_I, and T_G. Then the diffusion ranges can be denoted by $0 < t < T_L$ (local), $T_L < t < T_I$ (intermediate), $T_I < t < T_G$ (global), and $T_G < t$ (geomorphic). These crossover times are depicted as vertical lines in figure 2. To understand the scale dependence of bedload diffusion expressed by equation 15, we need

to determine the exponents γ of each range and express the crossover times T_L, T_I, and T_G in terms of the model parameters v, k_1, k_2, and κ.

The diffusion exponents γ in the local, intermediate, and global ranges can be determined from two limiting cases of equation (15): (1) $t \ll 1/\kappa$, and (2) $1/k_2 \to 0$ while $vk_2 = \text{const}$. Limit (1) corresponds to times so short that sediment burial has not had a chance to occur, while limit (2) corresponds to times so long that individual motions appear as instantaneous steps (having mean step length $l = vk_2$) (cf. H. A. Einstein, 1937). We evaluate these limits in appendix C and conclude that the scaling within the local range is $2 \leq \gamma \leq 3$ depending on the initial conditions θ_i. Within the intermediate range it is $\gamma = 1$. Finally, within the global range it is $2 \leq \gamma \leq 3$, depending on the parameters k_2, k_1, and κ. To summarize, when the timescale parameters of the model satisfy $k_2 \gg k_1 \gg \kappa$, it predicts local range superdiffusion, intermediate range normal diffusion, and global range superdiffusion.

The crossover times between local, intermediate, global, and geomorphic ranges that are depicted in figure 2 are defined by

$$T_L = \sqrt{\frac{1}{k_1}\frac{1}{k_2}}, \tag{16}$$

$$T_I = \sqrt{\frac{1}{k_1}\frac{1}{\kappa}}, \tag{17}$$

$$T_G = \sqrt{\frac{1}{\kappa}\frac{k_1 + k_2}{\kappa k_1}}. \tag{18}$$

Each of these is a geometric mean of two fundamental timescales of the model. The crossover T_L is a measure of the temporal length of smooth segments within bedload trajectories. A segment of a trajectory is said to be smooth if it has no sudden changes in velocity. According to Nikora (2002), if trajectories are smooth, we expect superdiffusion. Within our model, a trajectory can be expected to be smooth from $t = 0$ for either a time $1/k_1$, if a grain is at rest, or for a time $1/k_2$, if the grain is in motion. Since T_L is the geometric mean of these two possibilities, it seems reasonable that T_L characterizes the termination of local range superdiffusion. Similarly, the crossover T_I is the geometric mean of the average resting time $1/k_1$ and the average period required for sediment to become buried $1/\kappa$. The

We can infer from the classic flume tracer studies that normal diffusion is expected of bedload when the timescale of observation is not small enough to resolve individual motions (i.e., $t \gg 1/k_1$), nor is it large enough to resolve the loss of tracers due to sediment burial ($t \ll 1/\kappa$) (H. A. Einstein, 1937, 1942; Nakagawa & Tsujimoto, 1976; Yano, 1969).

Nikora (2002) originally associated the local range to the timescale "between two successive collisions with the bed", the intermediate range to the timescale of "tens or hundreds of collisions with the bed" or the time "between two successive rests" , and the global range as "consisting of many intermediate trajectories". Our interpretation of the ranges displayed in figure 2 differs from that of Nikora (2002). Our model does not explicitly include collisions. It includes only intervals of motion ($1/k_2$), intervals of rest ($1/k_1$), and intervals of rest until trapping by burial ($1/\kappa$). Similarly, but not quite identically to Nikora (2002), we associate local range superdiffusion to the The local range thus terminates at T_L given by equation (16) which is a geometric measure of the duration over which trajectories are typically smooth. We deviate further from Nikora (2002) with our concepts of the intermediate and global ranges of diffusion.

local range superdiffusion stems from the smoothness of bedload trajectories on relatively short timescales. A trajectory is called smooth when it does not have any sudden changes. In our model, there are two ways for a trajectory to be smooth. A grain can either be in motion without depositing (for a mean time $1/k_2$), or it can

be at rest without entraining (for a mean time $1/k_1$). From this perspective, it is reasonable that equation (16) characterizes the cessation of local range superdiffusion.

According to Nikora (2002), the intermediate range corresponds to the period between successive intervals of rest, which may involve. A typical timescale

The model we have presented reduces directly to earlier diffusion models in the same simplified limits used to extract the scaling exponents γ. As discussed in Appendix C, limit (1) leads directly to the model developed by Lisle et al. (1998) to describe soil transport within a sheet flow, while limit (2) implies identical diffusion as the active layer formulation of bedload transport gradually undergoing burial developed by Wu et al. (2019).

Their model generalizes the Einstein model, which is an infinite velocity diffusion model, to include a finite velocity and a statistical duration of motion. Although Lisle et al. (1998) only mention this anecdotally, this modification of H. A. Einstein (1937) leads to two stages of diffusion. Their model describes a local range superdiffusion and an intermediate range normal diffusion. Because it does not include any trapping process, it does not describe distinct diffusion characteristics in a global range. Limit (2) derives diffusion characteristics identical to those of . This model was based on an active layer formulation where sediment grains can be transferred from the active layer to a substrate layer with a constant probability per unit time.

To our knowledge, the model we have presented here is the first attempt to discern the scale dependence of bedload diffusion across local, intermediate, and global scales. We have derived three stages of diffusion and a late stage of no diffusion by making two generalizations to the H. A. Einstein (1937) model. First, we have promoted Einstein's instantaneous steps (with infinite velocity) to motions having finite velocities and durations. Second, we have included the possibility that sediment resting on the surface can become buried by sediment deposited from upstream.

This development gives us several key implications: First, The model confines the range over which normal diffusion of bedload is expected from below and above for the first time. When the timescale under consideration satisfies $T_L < t < T_I$, with T_L and T_I given by equations (16) and (17), we expect normal bedload diffusion $\sigma_x^2 = D_d t$. This heuristic may be useful to discern when and if simple stochastic models of bedload transport may be relevant to environmental science considerations such as contaminant transport (Macklin et al., 2006) or aquatic habitat restoration (e.g. Gaeuman, Stewart, Schmandt, & Pryor, 2017). Second, the model is a tool to link information about bedload diffusion across scales. In practice, we might measure sediment diffusion within a channel on one timescale with intent to apply our knowledge at longer or shorter timescales. For example, one could infer k_1 and k_2 by measuring the virtual velocity and diffusivity of sediment tracers within a channel in the intermediate range $T_L < t < T_I$ (e.g. Hassan & Bradley, 2017). In conjunction with an estimate of the trapping rate κ, equation 15 permits prediction of diffusion characteristics on the global range $T_I < t < T_G$, which is more difficult to study experimentally.

Finally, we highlight the limitations of the model we've presented and suggest some ideas for further research. First, bedload transport characteristics in real rivers are not spatially or temporally homogeneous. Channels morphology is known to strongly affect the transport characteristics of bedload tracers (e.g. Hassan & Bradley, 2017; Kasprak, Wheaton, Ashmore, Hensleigh, & Peirce, 2014), and the effect of varying flows on the mobility of sediment grains in natural channels is a significant impediment for stochastic models in the Einstein paradigm (Bradley & Tucker, 2012; Phillips, Martin, & Jerolmack, 2013). Since channel morphology also undergoes dynamic evolution, there is a perspective from which it's as if tracers are transporting within a random environment (cf. **?**). The mathematical framework we've drawn upon here,

which began with the CTRW of Montroll and Weiss (1965) and was developed into the multistate random walk by Weiss (1994); **?**, is an area of highly active research. To understand bedload diffusion, we should join this work. River science remains somewhat isolated from mainstream geophysics. We should draw it closer. Quote from einstein. bam

5 Conclusion

We have drawn on random walk theory developed for condensed matter physics in order to describe the three stages of bedload diffusion first noted by Nikora (2002); Nikora et al. (2001). By revisiting and generalizing the original bedload diffusion theory of H. A. Einstein (1937), we have put forth a model of bedload diffusion for bedload sediment undergoing burial. This derives four ranges of bedload diffusion across temporal scales and confines their scaling exponents. This implies a scale-dependent description of bedload diffusion which could be applied to environmental science problems. Given the ubiquity of anomalous transport across the sciences, we anticipate there are some other applications, perhaps in hydrology or contaminant transport, where such a mobile-immobile diffusion model with trapping from the immobile state might find application. We look forward to the exciting developments in Einstein's stochastic paradigm of river science which are sure to stem from this work.

A Calculation of the distribution function

Double transforming (1-3) using the definition (10) gives

$$\tilde{\omega}_{1T}(\eta,s) = \theta_1\tilde{g}_1(\eta,s) + \tilde{\omega}_2(\eta,s)\tilde{g}_1(\eta,s) - \tilde{\omega}_{1F}(\eta,s), \tag{A.1}$$
$$\tilde{\omega}_{1F}(\eta,s) = \theta_1\tilde{g}_1(\eta,s+\kappa) + \tilde{\omega}_2(\eta,s)\tilde{g}_1(\eta,s+\kappa), \tag{A.2}$$
$$\tilde{\omega}_2(\eta,s) \quad = \theta_2\tilde{g}_2(\eta,s) + \tilde{\omega}_{1F}(\eta,s)\tilde{g}_2(\eta,s). \tag{A.3}$$

This purely algebraic system solves for

$$\tilde{\omega}_{1T}(\eta,s) = \frac{\theta_1+\theta_2\tilde{g}_2(\eta,s)}{1-\tilde{g}_1(\eta,s+\kappa)\tilde{g}_2(\eta,s)}\big\{\tilde{g}_1(\eta,s) - \tilde{g}_1(\eta,s+\kappa)\big\}, \tag{A.4}$$
$$\tilde{\omega}_{1F}(\eta,s) = \frac{\theta_1+\theta_2\tilde{g}_2(\eta,s)}{1-\tilde{g}_1(\eta,s+\kappa)\tilde{g}_2(\eta,s)}\tilde{g}_1(\eta,s+\kappa), \tag{A.5}$$
$$\tilde{\omega}_2(\eta,s) \quad = \frac{\theta_2+\theta_1\tilde{g}_1(\eta,s+\kappa)}{1-\tilde{g}_1(\eta,s+\kappa)\tilde{g}_2(\eta,s)}\tilde{g}_2(\eta,s). \tag{A.6}$$

Double transforming (4-6) gives

$$\tilde{p}_0(\eta,s) = \frac{1}{s}\tilde{\omega}_{1T}(\eta,s), \tag{A.7}$$
$$\tilde{p}_1(\eta,s) = \theta_1\tilde{G}_1(\eta,s) + \tilde{\omega}_2(\eta,s)\tilde{G}_1(\eta,s), \tag{A.8}$$
$$\tilde{p}_2(\eta,s) = \theta_2\tilde{G}_2(\eta,s) + \tilde{\omega}_{1F}(\eta,s)\tilde{G}_2(\eta,s). \tag{A.9}$$

The total probability is $p(x,t) = p_0(x,t)+p_1(x,t)+p_2(x,t)$. Using equations (A.4-A.9) this becomes, in the double Laplace representation,

$$\tilde{p}(\eta,s) = \frac{1}{s}\frac{\theta_1+\theta_2\tilde{g}_2(\eta,s)}{1-\tilde{g}_1(\eta,s+\kappa)\tilde{g}_2(\eta,s)}\big\{\tilde{g}_1(\eta,s) - \tilde{g}_1(\eta,s+\kappa)\big\} + \frac{\theta_1\big[\tilde{G}_1(\eta,s) + \tilde{g}_1(\eta,s+\kappa)\tilde{G}_2(\eta,s)\big] + \theta_2\big[\tilde{G}_2(\eta,s) + \tilde{g}_2(\eta,s)\tilde{G}_1(\eta,s)\big]}{1-\tilde{g}_1(\eta,s+\kappa)\tilde{g}_2(\eta,s)}. \tag{A.10}$$

Plugging the propagators outlined in equations (8-9) into equation (A.10) gives

$$\tilde{p}(\eta, s) = \frac{1}{s} \frac{(s+\kappa+k')s + \theta_1(s+\kappa)\eta v + \kappa k_2}{(s+\kappa+k_1)\eta v + (s+\kappa+k')s + \kappa k_2}. \tag{A.11}$$

In this equation, $k' = k_1 + k_2$, and we have used the normalization requirement of the initial probabilities $\theta_1 + \theta_2 = 1$. The double inverse transform of this equation provides the distribution $p(x,t)$. It is convenient to invert the transform over η first. Using the results 15.103 (transform of exponential), 15.123 (transform of derivative), and 15.141 (transform of Dirac delta function) from Arfken (1985) provides

$$\begin{aligned}\tilde{p}(x, s) = \theta_1 \frac{s+\kappa}{s(s+\kappa+k_1)}\delta(x) + \frac{1}{v}\Big(&\frac{(s+\kappa+k')s + \kappa k_2}{s(s+\kappa+k_1)} \\ &- \frac{\theta_1(s+\kappa)[s(s+\kappa+k_1) + \kappa k_2]}{s(s+\kappa+k_1)^2}\Big) \exp\Big[- \frac{(s+\kappa+k')s + \kappa k_2}{s+\kappa+k_1}\frac{x}{v}\Big].\end{aligned} \tag{A.12}$$

Taking the remaining inverse transform over s, applying results 15.152 (substitution), 15.164 (translation), and 15.175 (transform of te^{kt}) from Arfken (1985), and defining the shorthand notations $\tau = k_1(t - x/v)$, $\xi = k_2 x/v$, and $\Omega = (\kappa + k_1)/k_1$, gives the simpler form

$$\begin{aligned}p(x,t) = \theta_1\Big[1 - \frac{k_1}{\kappa+k_1}\big(1 - e^{-(\kappa+k_1)t}\big)\Big]\delta(x) + \frac{1}{v}\exp[\Omega\tau - \xi] \\ \times \mathcal{L}^{-1}\Big\{\Big(\theta_2 + \frac{\theta_1 k_1 + \theta_2 k_2}{s} + \frac{\theta_1 k_1 k_2}{s^2} + \frac{\theta_2 \kappa k_2}{s(s-\kappa-k_1)} + \frac{\theta_1 \kappa k_1 k_2}{s^2(s-\kappa-k_1)}\Big) \\ \times \exp\big[\frac{k_1\xi}{s}\big]; \tau/k_1\Big\}.\end{aligned} \tag{A.13}$$

Using entries 2.2.2.1, 2.2.2.8, and 1.1.1.13 from Prudnikov, Brychkov, and Marichev (1992) in conjunction with the definition of the Marcum Q-function $\mathcal{P}_\mu(x,t)$ (e.g. Temme, 1996), and inserting the Heaviside functions to account for the fact that grains can neither travel backwards nor at speeds exceeding v, we finally arrive at equation 12 for the joint distribution $p(x,t)$.

B Calculation of the moments

We employ equation 11 to compute the first two moments of position x and ultimately its variance. The first two derivatives of the double Laplace transformed distribution (A.11) are

$$\partial_\eta \tilde{p}(\eta, s) = -v\frac{1}{s}\frac{[(s+\kappa+k')s + \kappa k_2][\theta_2(s+\kappa) + k_1]}{[\eta v(s+\kappa+k_1) + (s+\kappa+k')s + \kappa k_2]^2}, \tag{B.1}$$

$$\partial_\eta^2 \tilde{p}(\eta, s) = 2v^2\frac{1}{s}\frac{(s+\kappa+k_1)[(s+\kappa+k')s + \kappa k_2][\theta_2(s+\kappa) + k_1]}{[\eta v(s+\kappa+k_1) + (s+\kappa+k')s + \kappa k_2]^3}. \tag{B.2}$$

Evaluating these at $\eta = 0$ and applying equation (11) provides the Laplace transformed moments

$$\frac{\langle\tilde{x}(s)\rangle}{v} = \frac{1}{s}\frac{\theta_2(s+\kappa) + k_1}{(s+\kappa+k')s + \kappa k_2} = \frac{1}{s}\frac{\theta_2(s+\kappa) + k_1}{(s+a+b)(s+a-b)}, \tag{B.3}$$

$$\frac{\langle\tilde{x}^2(s)\rangle}{2v^2} = \frac{1}{s}\frac{(s+\kappa+k_1)(\theta_2(s+\kappa) + k_1)}{[(s+\kappa+k')s + \kappa k_2]^2} = \frac{1}{s}\frac{(s+\kappa+k_1)(\theta_2(s+\kappa) + k_1)}{(s+a+b)^2(s+a-b)^2}. \tag{B.4}$$

The parameters $a = (\kappa + k')/2$ and $b^2 = a^2 - \kappa k_2$ were introduced to factorize the denominators. These equations can be inverted using the properties 15.164 (translation), 15.11.1 (integration), and 15.123 (differentiation) from Arfken (1985) after expansion

in partial fractions. For the mean, the calculation is

$$\frac{2b}{v}\langle x\rangle = \big[\theta_2 + (k_1+\theta_2\kappa)\int_0^t dt\big]\mathcal{L}^{-1}\Big\{\frac{1}{s+a-b} - \frac{1}{s+a+b}; t\Big\} \tag{B.5}$$

$$= \Big[\theta_2 + \frac{k_1+\theta_2\kappa}{b-a}\Big]e^{(b-a)t} - \Big[\theta_2 - \frac{k_1+\theta_2\kappa}{a+b}\Big]e^{-(a+b)t} - \Big[\frac{k_1+\theta_2\kappa}{b-a} + \frac{k_1+\theta_2\kappa}{a+b}\Big]. \tag{B.6}$$

This equation rearranges to (13). The second moment (B.4) is

$$\frac{2b^2}{v^2}\langle x^2\rangle = \Big[\theta_2(\delta(t)+\partial_t) + (\theta_2(2\kappa+k_1)+k_1) + (\kappa+k_1)(\theta_2\kappa+k_1)\int_0^t dt\Big] \times \mathcal{L}^{-1}\Big\{\frac{1}{(s+a-b)^2} + \frac{1}{(s+a+b)^2} - \frac{1}{b(s+a-b)} + \frac{1}{b(s+a+b)}; t\Big\}. \tag{B.7}$$

This becomes

$$\frac{2b^3}{v^2}\langle x^2\rangle = \Big[\theta_2\partial_t + [\theta_2(2\kappa+k_1)+k_1] + (\kappa+k_1)(\theta_2\kappa+k_1)\int_0^t dt\Big] \times \Big((bt-1)e^{(b-a)t} + (bt+1)e^{-(a+b)t}\Big), \tag{B.8}$$

which evaluates to equation (14). The variance in equation (15) follows from $\sigma_x^2 = \langle x^2\rangle - \langle x\rangle^2$.

C Limiting behavior of the moments

The easiest approach to extract the earlier results of Wu et al. (2019), Lisle et al. (1998), and H. A. Einstein (1937) for the moments and positional variance as limiting cases is to use the Laplace transformed moments (B.3) and (B.4) as a starting point. An alternate approach is to take limits in the moments (13) and (14) directly, but this is somewhat challenging. First we obtain the Wu et al. (2019) model as a limit case. These authors accounted for sediment burial considering motions to be instantaneous. They characterized sediment movement by a thin-tailed step length distribution. This implicitly involves an infinite motion velocity. To obtain their conclusions on bedload diffusion, we send the mean duration of motion to zero, the velocity to infinity ($1/k_2 \to 0$ and $v \to \infty$), and we hold the mean step distance $l = v/k_2$ constant. We use the initial condition that grains start at rest ($\theta_1 = 1$). Enacting these limits in equations (B.3) and (B.4) provides

$$\langle\tilde{x}\rangle = k_1 l\frac{1}{s(s+\kappa)}, \tag{C.1}$$

$$\langle\tilde{x}^2\rangle = 2l^2k_1\frac{s+\kappa+k_1}{s(s+\kappa)^2}. \tag{C.2}$$

Inverting these equations and introducing the variables $c = lk_1$ (an effective velocity) and $D_d = l^2k_1$ (a diffusivity) provides positional variance

$$\sigma_x^2(t) = \frac{2D_d(1-e^{-\kappa t})}{\kappa} + \frac{(1-e^{-2\kappa t}-2e^{-\kappa t}\kappa t)c^2}{\kappa^2}. \tag{C.3}$$

This is mathematically identical to the key result of Wu et al. (2019), providing two ranges of diffusion when $\kappa \ll k_1$. One is normal and the other, induced by sediment burial, is superdiffusive. From here, the H. A. Einstein (1937) result can be obtained by turning off the burial process ($\kappa \to 0$):

$$\sigma_x^2(t) = 2D_d t. \tag{C.4}$$

This represents a single range of normal diffusion (cf. Hubbell & Sayre, 1964; Nakagawa & Tsujimoto, 1976).

The Lisle et al. (1998) result can be obtained similarly. For this case, we neglect the burial process ($\kappa \to 0$) but retain the finite velocity and motion duration in equations (B.3) and (B.4). For the initial condition $\theta_1 = 1$, this provides

$$\langle \tilde{x} \rangle = v k_1 \frac{1}{s^2(s + k')}, \tag{C.5}$$

$$\langle \tilde{x}^2 \rangle = 2v^2 k_1 \frac{s + k_1}{s^3(s + k')^2}. \tag{C.6}$$

Inverting these equations provides the variance when $t \ll 1/\kappa$:

$$\sigma_x^2 = 2v^2 \frac{k_1}{k'^4} \Big(k_1 \big[\frac{1}{2} - k' t e^{-k't} - \frac{1}{2} e^{-2k't} \big] + k_2 \big[-2 + k't + (2 + k't) e^{-k't} \big] \Big). \tag{C.7}$$

This result encodes two stages of diffusion: at small times there is superdiffusion $\sigma_x^2 \propto t^\gamma$ with $\gamma = 2 - 3$ depending on the initial condition, and at longer times there is normal diffusion. This links back to the Einstein model in the limit of instantaneous steps: $1/k_2 \to 0$ and $v \to \infty$ while $v/k_2 = l$.

Finally, we examine the limit $t \to 0$ while leaving $\kappa \neq 0$. This will highlight the effect of initial conditions on the local range superdiffusion. By applying Tauberian theorems, we can argue the $t \to 0$ variance is determined by the $s \to \infty$ limits of (B.3) and (B.4) (e.g. Weeks & Swinney, 1998; Weiss, 1994). Expanding these equations in powers of $1/s \ll 1$ and inverting the resulting transforms gives

$$\langle x \rangle = v\theta_2 t + \frac{1}{2} v(\theta_1 k_1 - \theta_2 k_2) t^2 + O(t^3), \tag{C.8}$$

$$\langle x^2 \rangle = v^2 \theta_2 t^2 + \frac{1}{3} v^2 (\theta_1 k_1 - 2\theta_2 k_2) t^3 + O(t^4). \tag{C.9}$$

Taking only leading order terms for each option of θ_1 and θ_2, these equations provide the asymptotic ($t \to 0$) variance

$$\sigma_x^2(t) \sim v^2 \theta_1 \theta_2 t^2 + \frac{1}{3} v^2 (\theta_1 k_1 + \theta_2 k_2) t^3. \tag{C.10}$$

This equation shows the effect of initial conditions on the diffusion characteristics of the local range.

Acknowledgments

J. Pierce acknowledges helpful exchanges with Eduardo Daly and Peter Hänggi during the early stages of this work. He would like to thank Melinda Saunders and Leonardo Golubovic for their careful guidance in mathematics through the years. M. Hassan is supported by an NSERC Discovery grant. The Python simulation code is available at `https://github.com/kevinkayaks/rw-diffu`.

References

Aarão Reis, F. D., & Di Caprio, D. (2014). Crossover from anomalous to normal diffusion in porous media. *Physical Review E - Statistical, Nonlinear, and Soft Matter Physics*, *89*(6), 1–10. doi: 10.1103/PhysRevE.89.062126

Arfken, G. (1985). *Mathematical Methods for Physicists*. Academic Press, Inc. doi: 10.1063/1.3062258

Balakrishnan, V., & Chaturvedi, S. (1988). Persistent Diffusion on a Line. *Physica A*, *148*, 581–596.

Barik, D., Ghosh, P. K., & Ray, D. S. (2006). Langevin dynamics with dichotomous noise; Direct simulation and applications. *Journal of Statistical Mechanics: Theory and Experiment*(3). doi: 10.1088/1742-5468/2006/03/P03010

Bena, I. (2006). Dichotomous Markov noise: Exact results for out-of-equilibrium systems. A review. *International Journal of Modern Physics B*, *20*(20), 2825–2888. Retrieved from http://arxiv.org/abs/cond-mat/0606116{\%}0Ahttp://dx.doi.org/10.1142/S0217979206034881 doi: 10.1142/S0217979206034881

Berezhkovskii, A. M., & Weiss, G. H. (2002). Detailed description of a two-state non-Markov system. *Physica A: Statistical Mechanics and its Applications*, *303*(1-2), 1–12. doi: 10.1016/S0378-4371(01)00431-9

Berkowitz, B., Cortis, A., Dentz, M., & Scher, H. (2006). Modeling Non-fickian transport in geological formations as a continuous time random walk. *Reviews of Geophysics*, *44*(2), 1–49. doi: 10.1029/2005RG000178

Bialik, R. J., Nikora, V. I., & Rowiński, P. M. (2012). 3D Lagrangian modelling of saltating particles diffusion in turbulent water flow. *Acta Geophysica*, *60*(6), 1639–1660. doi: 10.2478/s11600-012-0003-2

Bradley, N. D. (2017). Direct Observation of Heavy-Tailed Storage Times of Bed Load Tracer Particles Causing Anomalous Superdiffusion. *Geophysical Research Letters*, *44*(24), 12,227–12,235. doi: 10.1002/2017GL075045

Bradley, N. D., & Tucker, G. E. (2012). Measuring gravel transport and dispersion in a mountain river using passive radio tracers. *Earth Surface Processes and Landforms*, *37*, 1034–1045. doi: 10.1002/2017GL075045

Daly, E., & Porporato, A. (2010). Effect of different jump distributions on the dynamics of jump processes. *Physical Review E - Statistical, Nonlinear, and Soft Matter Physics*, *81*(6), 1–10. doi: 10.1103/PhysRevE.81.061133

Einstein, A. (1905). Brownian Movement. *Biotropica*, *1*. doi: 10.5167/uzh-53657

Einstein, H. A. (1937). *Bed-load transport as a probability problem* (Unpublished doctoral dissertation). ETH Zurich.

Einstein, H. A. (1942). Formulas for the transportation of bed load. *Transactions of the A.S.C.E.*, *106*, 561–597. doi: 10.1061/(ASCE)HY.1943-7900.0001248.

Fan, N., Singh, A., Guala, M., Foufoula-Georgiou, E., & Wu, B. (2016). Exploring a semimechanistic episodic Langevin model for bed load transport: Emergence of normal and anomalous advection and diffusion regimes. *Water Resources Research*, *52*(4), 3787–3814. doi: 10.1002/2016WR018704.Received

Flekkøy, E. G. (2017). Minimal model for anomalous diffusion. *Physical Review E*, *95*(1), 1–6. doi: 10.1103/PhysRevE.95.012139

Frey, P. (2014). Particle velocity and concentration profiles in bedload experiments on a steep slope. *Earth Surface Processes and Landforms*, *39*(5), 646–655. doi: 10.1002/esp.3517

Gaeuman, D., Stewart, R., Schmandt, B., & Pryor, C. (2017). Geomorphic response to gravel augmentation and high-flow dam release in the Trinity River, California. *Earth Surface Processes and Landforms*, *42*(15), 2523–2540. doi: 10.1002/esp.4191

Giddings, J. C., & Eyring, H. (1955). A molecular dynamic theory of chromatography. *Journal of Physical Chemistry*, *59*(5), 416–420.

Gordon, R., Carmichael, J. B., & Isackson, F. J. (1972). Saltation of Plastic Balls in a 'One-Dimensional' Flume. *Water Resources Research*, *8*(2), 444–458. doi: 10.1029/WR008i002p00444

Hassan, M. A., & Bradley, D. N. (2017). Geomorphic controls on tracer particle dispersion in gravel bed rivers. In *Gravel-bed rivers: Processes and disasters* (pp. 159–184). New York, NY: John Wiley & Sons Ltd. doi: 10.16719/j.cnki.1671-6981.2015.03.007

Hassan, M. A., & Church, M. (1994). Vertical mixing of coarse particles in gravel bed rivers: A kinematic model. *Water Resources Research*, *30*(4), 1173–1185. doi: 10.1029/93WR03351

Hassan, M. A., Church, M., & Schick, A. P. (1991). Distance of movement of coarse particles in gravel bed streams. *Water Resources Research*, *27*(4), 503–511.

doi: 10.1029/90WR02762

Hubbell, D. W., & Sayre, W. W. (1964). Sand Transport Studies with Radioactive Tracers. *J. Hydr. Div.*, *90*(HY3), 39–68.

Jeon, J. H., Monne, H. M. S., Javanainen, M., & Metzler, R. (2012). Anomalous diffusion of phospholipids and cholesterols in a lipid bilayer and its origins. *Physical Review Letters*, *109*(18), 1–5. doi: 10.1103/PhysRevLett.109.188103

Kasprak, A., Wheaton, J. M., Ashmore, P. E., Hensleigh, J. W., & Peirce, S. (2014). The relationship between particle travel distance and channel morphology : Results from physical models of braided rivers. *Journal of Geophysical Research : Earth Surface*, *120*, 55–74. doi: 10.1002/2014JF003310.Received

Kittel, C. (1958). *Elementary Statistical Physics*. R.E. Krieger Pub. Co.

Lajeunesse, E., Malverti, L., & Charru, F. (2010). Bed load transport in turbulent flow at the grain scale: Experiments and modeling. *Journal of Geophysical Research: Earth Surface*, *115*(4). doi: 10.1029/2009JF001628

Lisle, I. G., Rose, C. W., Hogarth, W. L., Hairsine, P. B., Sander, G. C., & Parlange, J.-Y. (1998). Stochastic sediment transport in soil erosion. *Journal of Hydrology*, *204*, 217–230.

Macklin, M. G., Brewer, P. A., Hudson-Edwards, K. A., Bird, G., Coulthard, T. J., Dennis, I. A., ... Turner, J. N. (2006). A geomorphological approach to the management of rivers contaminated by metal mining. *Geomorphology*, *79*(3-4), 423–447. doi: 10.1016/j.geomorph.2006.06.024

Marcum, J. (1960). A statistical theory of target detection by pulse radar. *IRE Trans. Inform. Theory*, *6*, 59–268.

Martin, R. L., Jerolmack, D. J., & Schumer, R. (2012). The physical basis for anomalous diffusion in bed load transport. *Journal of Geophysical Research: Earth Surface*, *117*(1), 1–18. doi: 10.1029/2011JF002075

Martin, R. L., Purohit, P. K., & Jerolmack, D. J. (2014). Sedimentary bed evolution as a mean-reverting random walk: Implications for tracer statistics. *Geophysical Research Letters*, *41*(17), 6152–6159. doi: 10.1002/2014GL060525

Metzler, R., & Klafter, J. (2000). The random walk's guide to anomalous diffusion: A fractional dynamics approach. *Physics Report*, *339*(1), 1–77. doi: 10.1016/S0370-1573(00)00070-3

Molina-Garcia, D., Sandev, T., Safdari, H., Pagnini, G., Chechkin, A., & Metzler, R. (2018). Crossover from anomalous to normal diffusion: Truncated power-law noise correlations and applications to dynamics in lipid bilayers. *New Journal of Physics*, *20*(10). doi: 10.1088/1367-2630/aae4b2

Montroll, E. W., & Weiss, G. H. (1965). Random Walks on Lattice. II. *Jounral of Mathematical Physics*, *6*, 167–181.

Nakagawa, H., & Tsujimoto, T. (1976). On Probabilistic Characteristics of Motion of Individual Sediment Particles on Stream Beds. In *Hydraulic problems solved by stochastic methods: Second international iahr symposium on stochastic hydraulics* (pp. 293–320). Lund, Sweden.

Nakagawa, H., & Tsujimoto, T. (1980). Sand bed instability due to bed load motion. *Journal of the Hydraulics Division-ASCE*.

Nikora, V. (2002). On bed particle diffusion in gravel bed flows under weak bed load transport. *Water Resources Research*, *38*(6), 1–9. Retrieved from `http://doi.wiley.com/10.1029/2001WR000513` doi: 10.1029/2001WR000513

Nikora, V., Heald, J., Goring, D., & McEwan, I. (2001). Diffusion of saltating particles in unidirectional water flow over a rough granular bed. *Journal of Physics A: Mathematical and General*, *34*(50). doi: 10.1088/0305-4470/34/50/103

Phillips, C. B., Martin, R. L., & Jerolmack, D. J. (2013). Impulse framework for unsteady flows reveals superdiffusive bed load transport. *Geophysical Research Letters*, *40*(7), 1328–1333. doi: 10.1002/grl.50323

Prudnikov, A., Brychkov, Y. A., & Marichev, O. (1992). *Integrals and Series: Volume 5: Inverse Laplace Transforms*. Gordon and Breach Science Publishers.

Reynolds, A., & Rhodes, C. (2009). The Levy flight paradigm: random search patterns and mechanisms. *Ecology*, *90*(4), 877–887.

Schmidt, M. G., Sagués, F., & Sokolov, I. M. (2007). Mesoscopic description of reactions for anomalous diffusion: A case study. *Journal of Physics Condensed Matter*, *19*(6). doi: 10.1088/0953-8984/19/6/065118

Sokolov, I. M. (2012). Models of anomalous diffusion in crowded environments. *Soft Matter*, *8*(35), 9043–9052. doi: 10.1039/c2sm25701g

Taylor, G. I. (1920). Diffusion by continuous movements. *Proceedings of the London Mathematical Society*, *s2-20*(1), 196–212.

Temme, N. M. (1996). *Special functions: an introduction to the classical functions of mathematical physics*. John Wiley & Sons Ltd.

Vallaeys, V., Tyson, R. C., Lane, W. D., Deleersnijder, E., & Hanert, E. (2017). A Lévy-flight diffusion model to predict transgenic pollen dispersal. *Journal of the Royal Society Interface*, *14*(126). doi: 10.1098/rsif.2016.0889

Voepel, H., Schumer, R., & Hassan, M. A. (2013). Sediment residence time distributions: Theory and application from bed elevation measurements. *Journal of Geophysical Research: Earth Surface*, *118*(4), 2557–2567. doi: 10.1002/jgrf.20151

Weeks, E. R., & Swinney, H. L. (1998). Anomalous diffusion resulting from strongly asymmetric random walks. *Physical Review E - Statistical Physics, Plasmas, Fluids, and Related Interdisciplinary Topics*, *57*(5), 4915–4920. doi: 10.1103/PhysRevE.57.4915

Weiss, G. H. (1976). The two-state random walk. *Journal of Statistical Physics*, *15*(2), 157–165. doi: 10.1007/BF01012035

Weiss, G. H. (1994). *Aspects and applications of the random walk*. Amsterdam: North Holland.

Wu, Z., Foufoula-Georgiou, E., Parker, G., Singh, A., Fu, X., & Wang, G. (2019). Analytical Solution for Anomalous Diffusion of Bedload Tracers Gradually Undergoing Burial. *Journal of Geophysical Research: Earth Surface*, *124*(1), 21–37. doi: 10.1029/2018JF004654

Yang, C. T., & Sayre, W. W. (1971). Stochastic model for sand dispersion. *Journal of the Hydraulics Division, ASCE*, *97*(HY2).

Yang, X. R., & Wang, Y. (2019). Ubiquity of anomalous transport in porous media: Numerical evidence, continuous time random walk modelling, and hydrodynamic interpretation. *Scientific Reports*, *9*(1), 1–11. Retrieved from `http://dx.doi.org/10.1038/s41598-019-39363-3` doi: 10.1038/s41598-019-39363-3

Yano, K. (1969). Tracer Studies on the Movement of Sand and Gravel. In *Proceedings of the 12th congress iahr, vol 2.* (pp. 121–129). Kyoto, Japan.

Zhang, Y., Meerschaert, M. M., & Packman, A. I. (2012). Linking fluvial bed sediment transport across scales. *Geophysical Research Letters*, *39*(20), 1–6. doi: 10.1029/2012GL053476